Electronic Supplementary Material (ESI) for CrystEngComm.

Influences of As(V), Sb(III), and Hg(II) Ions on the Nucleation and Growth of Akaganeite

Verónica Villacorta,*[a] Karen Edilma García, [a] Jean-Marc Greneche,[b] and César Augusto Barrero[a]

*Corresponding authors

[a]Solid State Group, Faculty of Exact and Natural Sciences, University of Antioquia – UdeA. Medellín, Street 67 N°53-108, Colombia.

E-mail vvillacortal@unal.edu.co; karen.garcia@udea.edu.co

[b]Institut des Molécules et Matériaux du Mans – IMMM UMR CNRS 6283. Université du Maine. Le Mans, 72085, France

SUPPORTING INFORMATION

XRD Analysis. X-ray diffraction (XRD) analysis was performed using a Panalytical Empyream Serie 2 X-ray diffractometer. The powder pattern was obtained using a Co-Kα radiation. The equipment operated with a scan range from 5° to 80°, a scan step size of 0.013° and a time per step of 59.670 s. The diffractograms were analyzed using a program based on the Rietveld methodology and Fourier transform called MAUD[42] through which the values of scale factor, sample displacement, incident intensity, unit cell parameters, six-order polynomial background, and the average crystallite size were refined. The average crystallite size and texture were assumed to be anisotropic. The Rietveld analysis was performed using the CIF file of akaganeite with the monoclinic symmetry I2/m (COD code 9001319).[43]

XRF Analysis. X-ray fluorescence (XRF) analysis was performed using a Thermo Scientific ARL OPTIM´X by wavelength dispersive x-ray fluorescence (WDXRF).

TEM and STEM. High-resolution transmission electron microscopy (TEM) and Scanning transmission electron microscopy analysis were performed with a FEI Tecnai G2 F20 Super-Twin transmission electron microscope operating at 200 kV. The preparation of the sample consisted of the dilution in ethanol of a small amount of the same, followed by the immersion of the mixture in an ultrasonic bath, in order to disperse the sample in the solvent. Finally, the analysis was carried out by depositing a drop of the dispersion on a Cu grid coated with a carbon film.

Raman spectroscopy. Raman spectra were obtained with a Horiba Confocal Raman Spectrometer Yvon, High Resolution Labram HR Model, equipped with a He/Ne laser operating at 632.81 nm and a Nicon confocal microscope model BX-41 provided with lenses of 50X. The helium - neon laser was focused to a spot size of 1-2 μm^2 at the samples. The scattered light was dispersed by a monochromator with 600 lines/mm grating and detected by a CCD system with resolution of 1024 x 256 pixels. The spectra range was from 100 to 4000 cm^{-1}, with a step size of 1.1 cm^{-1}. Moreover, the acquisition time was of 30 s with an accumulation of 2x5. The hold and slit were of 800 µm and 600 µm, respectively. Finally, with the objective of avoiding any transformation of the samples, the influence of the laser power was previously tested. In this way, it was concluded that the use of the D0.6 filter, which reduced the power to 0.85 mW, was the ideal for treating the samples. The Raman experiments were performed to the samples and its respective replicates, with the aim of confirming the reproducibility of all syntheses. In addition, to verify sample homogeneity the spectra collection was carried out repeatedly at different colored regions of each synthesis and each replicate, with the objective of confirming the existence or absence of other phases. Pure akaganeite appeared homogeneously red colored and the rest of the samples showed regions of red, white and dark colors. However, all repeated spectra showed to be identical and independent of color variation. All Raman spectral data were baseline-corrected and curve-fitted to obtain quantitative information of the band parameters like wavenumbers, widths, and relative intensities. All spectra were adjusted with Lorentzians lines as proposed in previous studies and obtained correlation coefficients r^2 higher than 0.98. It is important to note that Raman spectra were conveniently delimited in different regions in function of the excited vibrations in the structure in order to obtain the best fit in each case.

Infrared spectroscopy. A Perkin-Elmer model 1000 FTIR spectrometer was used for infrared (IR) spectra collection. The sample scans ranged from 400 to 4000 cm^{-1} with 4 cm^{-1} resolution. Some regions of the IR spectra were curve-fitted to obtain quantitative information on the wavenumbers, widths, and relative intensities. For that purpose, we used Lorentzians lines and obtained correlation coefficients r^2 higher than 0.98.

Mössbauer spectroscopy. The transmission Mössbauer spectra were recorded at 300 K and 77 K using a 25 mCi ^{57}Co in rhodium source. Mössbauer spectra were collected in a time-mode spectrometer working in the transmission geometry using a constant acceleration drive with triangular reference signal. Calibration was achieved from standard α-iron foil at 300 K. The spectra were analyzed using a home-made program called MOSFIT which is based on non-linear least squares fitting procedures assuming Lorentzian Mössbauer lines while the values of isomer shift are quoted to that of α -Fe at 300 K.

Table SI_1. Amount of antimony, arsenic, iron and chloride present in the structure of samples co-precipitated with 60 ppm of the pollutants as determined by XRF. Only the amount of mercury was determined by STEM.

Element	Weight (%)	Element	Weight (%)	Element	Weight (%)
Hg	0.94 ± 0.01	**Sb**	1.41 ± 0.05	**As**	3.51 ± 0.08
Fe	65.53 ± 0.09	**Fe**	62.59 ± 0.11	**Fe**	63.50 ± 0.10
Cl	5.64 ± 0.12	**Cl**	7.25 ± 0.13	**Cl**	3.82 0.10

Table SI_2. Percentage distribution dissolved species of Hg^{2+}, Sb^{3+} and As^{5+} in the reaction medium at room temperature (25°C). In all experiments, the concentration of $FeCl_3 \cdot 6H_2O$ was fixed at 0.05M, while the concentrations of pollutants were fixed at 60ppm of Hg(II), Sb(III) and As(V). The pH was 1.19 for combined solution of $FeCl_3$ and Hg^{2+}, 0.96 for combined solution of $FeCl_3$ and Sb^{3+} and 1.59 for combined solution of $FeCl_3$ and As^{5+}. Only the most abundant species are listed.

Component	**Species name**	**Total concentration (%)**	**Component**	**Species name**	**Total concentration (%)**	**Component**	**Species name**	**Total concentration (%)**
$Hg(OH)_2$	$HgCl_2$ (aq)	63.608	**$Sb(OH)_3$**	$Sb(OH)_2^+$	79.37	**AsO_4^{3-}**	H_3AsO_4	80.722
	$HgCl_3^{1-}$	27.922		$Sb(OH)_3$	20.63		$H_2AsO_4^-$	19.278
Cl^{1-}	Cl^{1-}	82.583	**Cl^{1-}**	Cl^{1-}	83.867	**Cl^{1-}**	Cl^{1-}	84.432
	$FeCl_2^+$	15.948		$FeCl_2^+$	16.133		$FeCl_2^+$	15.568
Fe^{3+}	Fe^{3+}	80.36	**Fe^{3+}**	Fe^{3+}	81.971	**Fe^{3+}**	Fe^{3+}	74.748
	$FeCl_2^+$	15.948		$FeCl_2^+$	16.134		$FeCl_2^+$	15.569
	$Fe(OH)_2^+$	2.592		$Fe(OH)_2^+$	1.511		$Fe(OH)_2^+$	5.248

Table SI_3. Evolution of a, b, c, and β parameters, unit cell volume and mean crystallize size with the increase of Hg^{2+}, Sb^{3+} and As^{5+} concentrations.

Sample	**a [Å]**	**b [Å]**	**c [Å]**	**β**	**Cell volume [Å^3]**	**Mean crystallize size [nm]**
pAk	10,5083 ±0,0012	3,0217 ±0,0003	10,4972 ±0,0012	89,975 ±0,012	301,616 ±0,0003	134 ±19
Ak0.25Hg	10,5001 ±0,0035	3,0214 ±0,0002	10,4991 ±0,0035	90,061 ±0,015	288,207 ±0,0007	93 ±16
Ak5Hg	10,5066 ±0,0034	3,0204 ±0,001	10,4910 ±0,0039	90,006 ±0,033	296,681 ±0,001	76 ±8
Ak20Hg	10,5247 ±0,0044	3,0233 ±0,0013	10,4866 ±0,0044	90,025 ±0,019	294,52 ±0,0012	38 ±3
Ak60Hg	10,5023 ±0,0060	3,0150 ±0,0018	10,4343 ±0,0061	89,879 ±0,023	311,097 ±0,0017	20 ±1
Ak0.25Sb	10,5129 ±0,0024	3,0226 ±0,0007	10,5021 ±0,0022	89,990 ±0,014	299,805 ±0,001	94 ±6
Ak10Sb	10,5224 ±0,0105	3,0214 ±0,0006	10,4982 ±0,0023	90,019 ±0,017	295,497 ±0,001	86 ±11
Ak20Sb	10,4927 ±0,0022	3,0128 ±0,0021	10,4563 ±0,0076	90,063 ±0,050	285,560 ±1,001	33 ±3
Ak60Sb	10,4970 ±0,0078	3,0086 ±0,0023	10,3999 ±0,0079	90,242 ±0,04	249,726 ±0,002	17 ±1
Ak0.25As	10,5035 ±0,0046	3,0203 ±0,0007	10,5032 ±0,0031	89,999 ±0,015	298,105 ±0,001	82 ±19
Ak5As	10,4932 ±0,0029	3,0225 ±0,0009	10,5248 ±0,003	90,058 ±0,019	289,318 ±0,001	54 ±4
Ak20As	10,4762 ±0,0043	3,0218 ±0,0013	10,5235 ±0,0045	90,037 ±0,031	292,141 ±0,001	41 ±6
Ak60As	10,4444 ±0,0102	2,9958 ±0,0029	10,3564 ±0,013	89,981 ±0,072	292,458 ±0,003	13 ±2

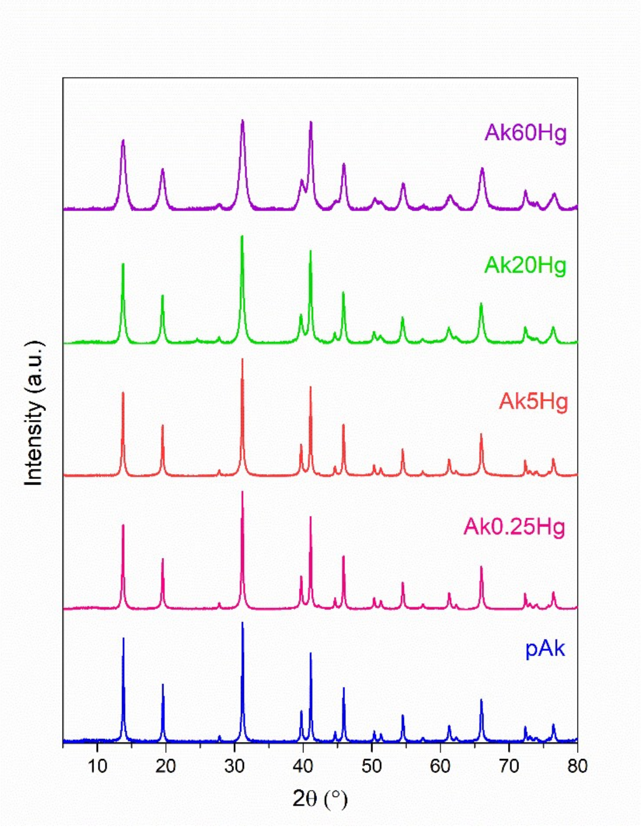

Figure SI_1. X-ray diffraction patterns of the samples co-precipitated in the presence of varying concentrations of Hg^{2+}.

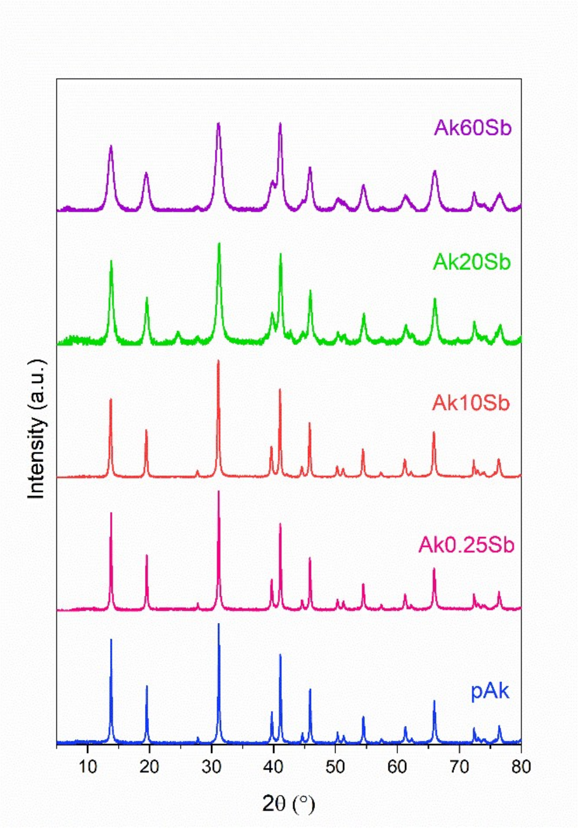

Figure SI_2. X-ray diffraction patterns of the samples co-precipitated in the presence of varying concentrations of Sb^{3+}.

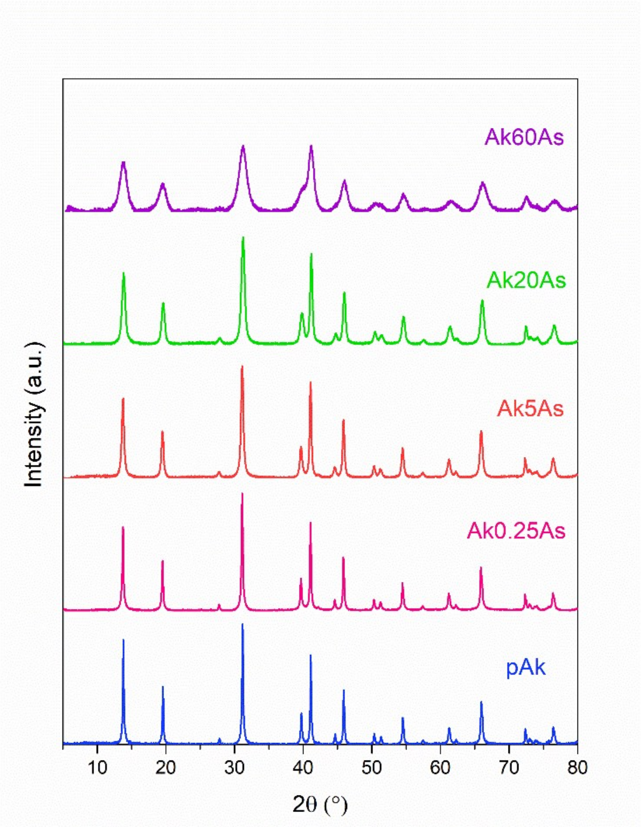

Figure SI_3. X-ray diffraction patterns of the samples co-precipitated in the presence of varying concentrations of As^{5+}.

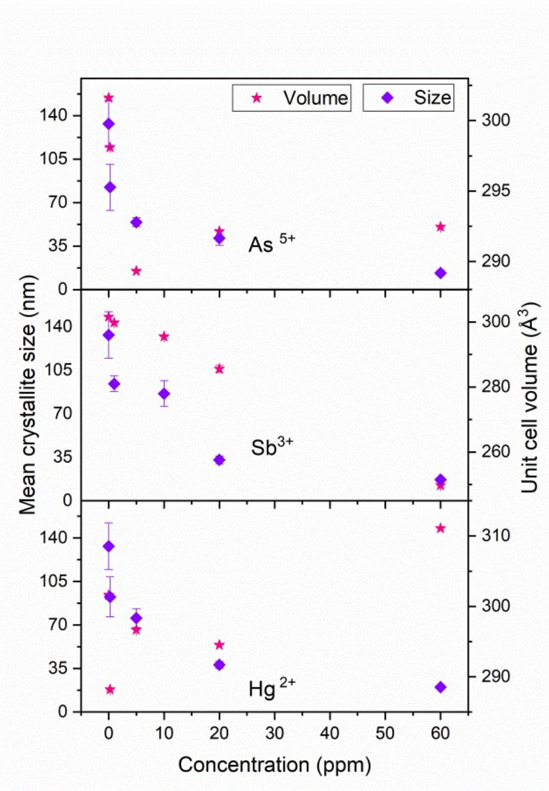

Figure SI_4. Variations of the mean crystallite sizes (purple diamond) and unit cell volumes (pink star) with the pollutant concentration for akaganeite co-precipitated with Hg^{2+} (bottom), Sb^{3+} (middle) and As^{5+}.

Table SI_4. Comparison of the wavenumbers (in cm^{-1}) of the principal bands observed in the Raman spectrum of pure akaganeite in this study with some data reported in the literature. The data are divided into two wavenumber regions: low and high.

	Low wavenumber region (100 - 1800 cm^{-1})	**High wavenumber region (3000 - 4000 cm^{-1})**
This study	137, 310, 386, 491, 541, 600, 720, 886, 1149, broad band centered at about 1361.	3296, 3368, 3426, 3523
Oh and co-worker[51]	314, 380, 549, 722	Non reported
Das and Hendry[52]	314, 400, 550, 720	Non reported
Richmond and co-workers[25]	137, 307, 387, 535, 597, 719, 906	Non reported
Réguer and co-workers[3]	310, 390, 490, 540, 610, 720, 930, 1160, broad band from 1300 to 1500.	3242, 3360, 3422, 3530

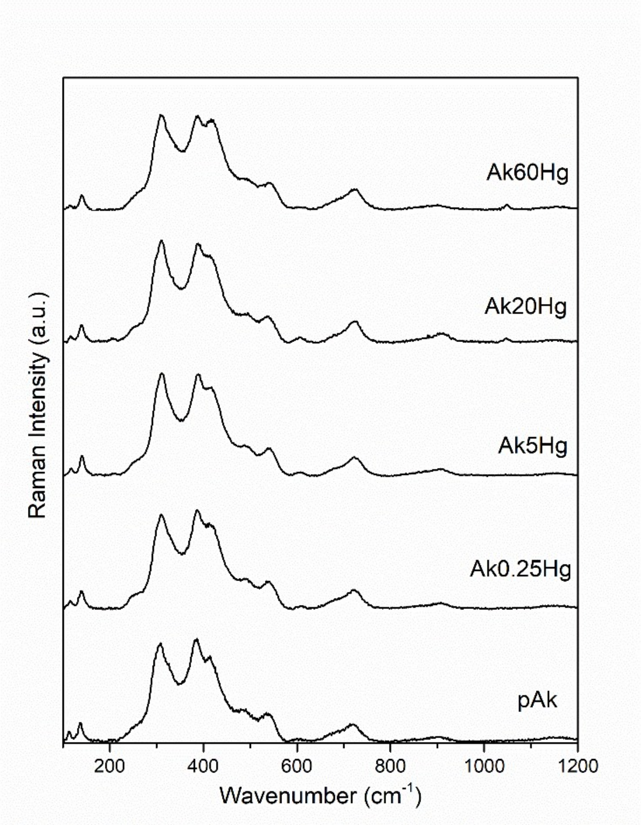

Figure SI_5. Raman spectra of pAk, Ak0.25Hg, Ak5Hg, Ak20Hg and Ak60Hg in the wavenumber region from 100 to 1200 cm^{-1}.

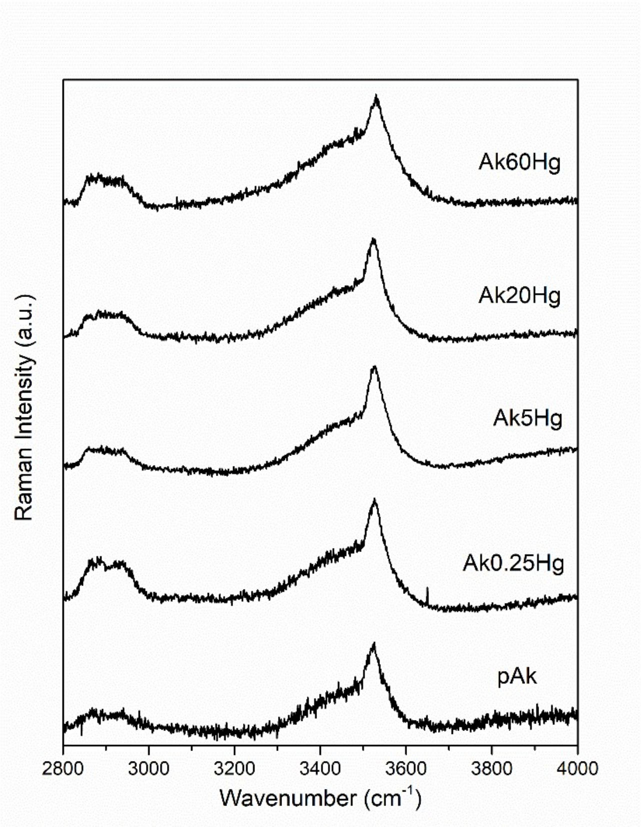

Figure SI_6. Raman spectra of pAk, Ak0.25Hg, Ak5Hg, Ak20Hg and Ak60Hg in the wavenumber region from 2800 to 4000 cm^{-1}.

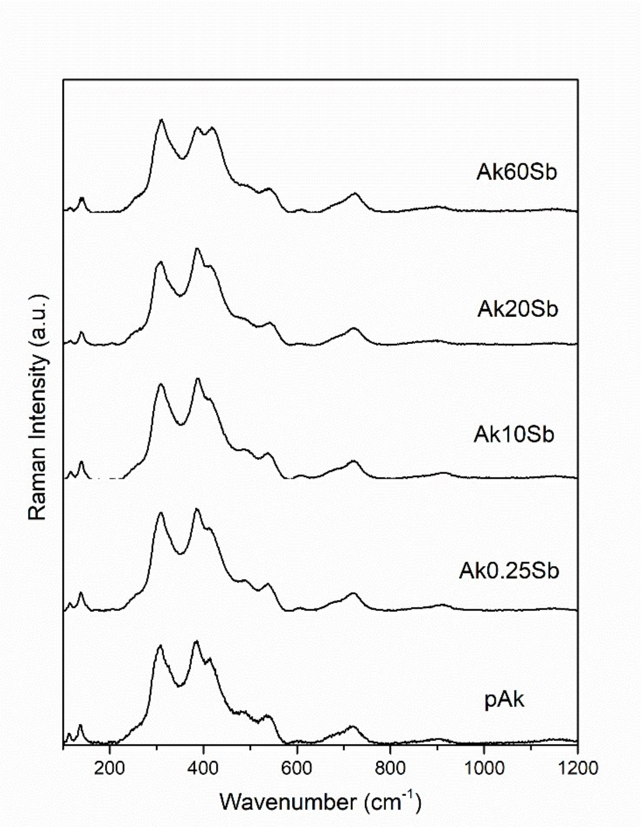

Figure SI_7. Raman spectra of pAk, Ak0.25Sb, Ak10Sb, Ak20Sb and Ak60Sb in the wavenumber region from 100 to 1200 cm^{-1}.

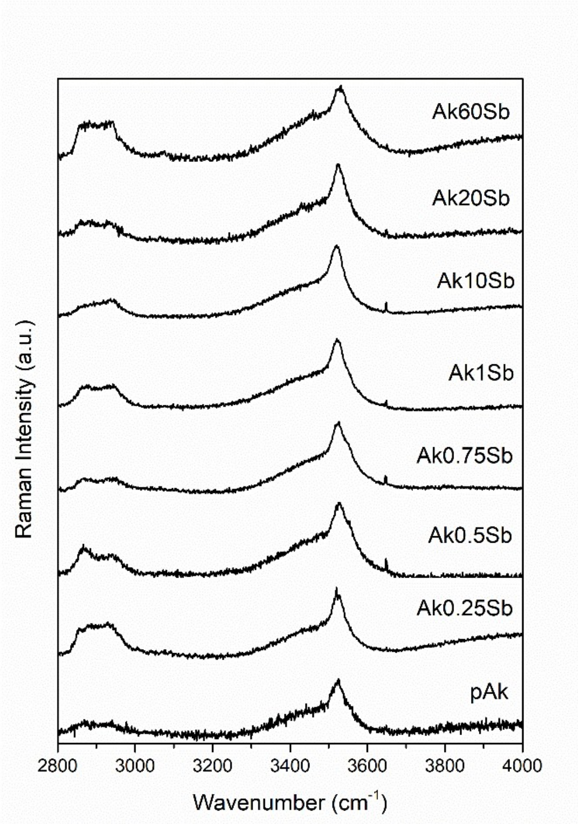

Figure SI_8. Raman spectra of pAk, Ak0.25Sb, Ak0.5Sb, Ak0.75Sb, Ak1Sb, Ak10Sb, Ak20Sb and Ak60Sb in the wavenumber region from 2800 to 4000 cm^{-1}.

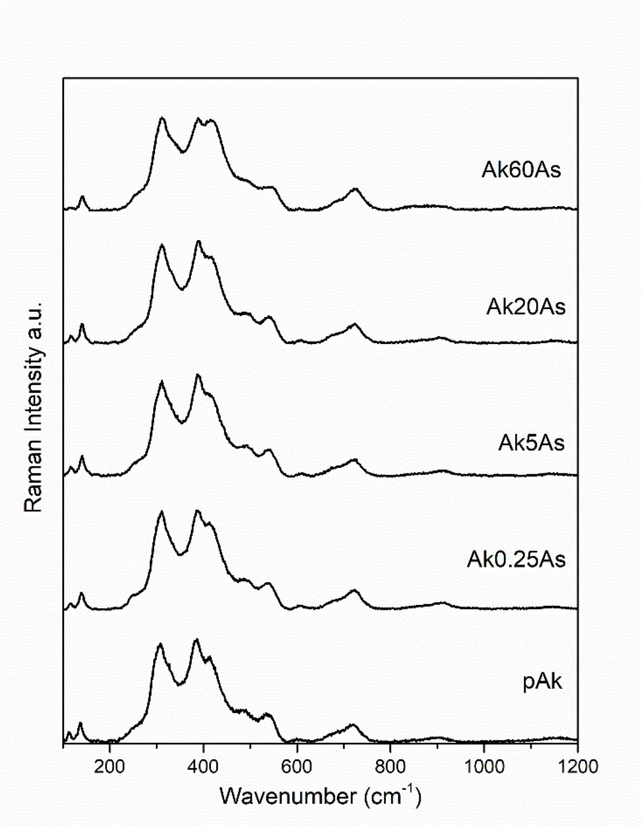

Figure SI_9. Raman spectra of pAk, Ak0.25As, Ak5As, Ak20As and Ak60As in the wavenumber region from 100 to 1200 cm^{-1}.

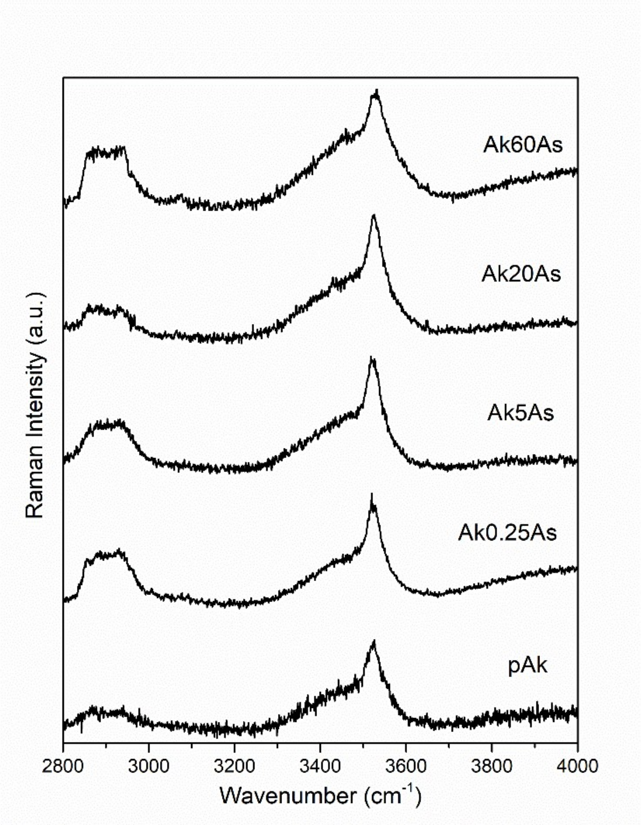

Figure SI_10. Raman spectra of pAk, Ak0.25As, Ak5As, Ak20As and Ak60As in the wavenumber region from 2800 to 4000 cm^{-1}.

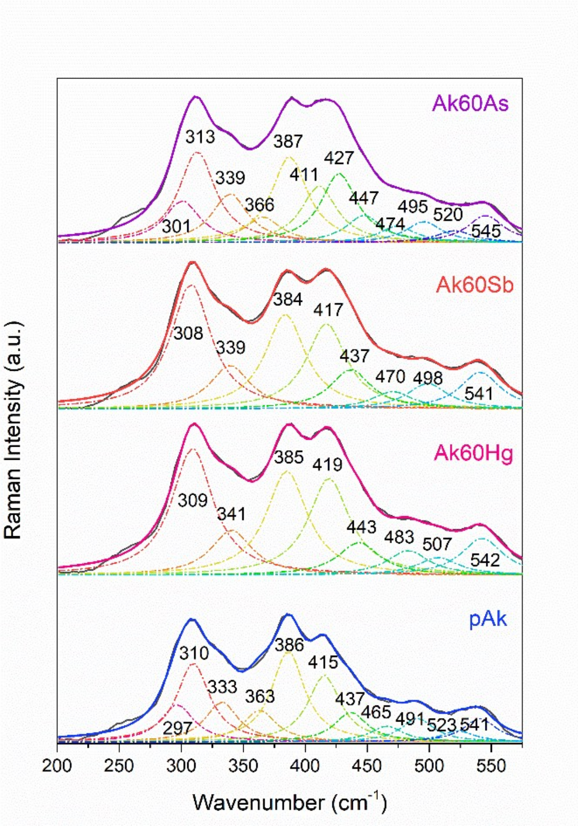

Figure SI_11. Decomposition of Raman spectra for pAk, Ak60Hg, Ak60Sb and Ak60As in the wavenumber region from 200 to 600 cm^{-1}.

Table SI_5. Wavenumbers and integrated areas of the Raman bands localized from 200 to 600 cm^{-1} corresponding to the pure and co-precipitated akaganeites with 60 ppm of Hg^{2+}, Sb^{3+} and As^{5+}. The relative intensity ratio of the two Raman bands located at about 310 and 330 cm^{-1} for each spectrum is also reported and the calculated chlorine content according to Figure 4 of the paper by Réguer and co-workers.[3]

Sample	Wavenumbers [cm^{-1}]	Integrated area [%]	Relative intensity ratio of selected paired bands	Cl content (% mass) using data from Réguer *et al.*[3]
pAk	297 ± 3	11 ± 4	$\frac{I_{310}}{I_{333}} = \frac{67}{33}$	**9 – 10**
	310 ± 2	24 ± 4		
	333 ± 1	12 ± 1		
	363 ± 2	10 ± 1		
	386 ± 1	27 ± 1		
	415 ± 1	20 ± 1		
	437 ± 2	9 ± 1		
Ak60Hg	309 ± 1	39 ± 1	$\frac{I_{309}}{I_{341}} = \frac{74}{26}$	Not graphed
	341 ± 1	14 ± 1		
	385 ± 1	32 ± 1		
	419 ± 1	30 ± 1		
	443 ± 2	10 ± 1		
Ak60Sb	308 ± 1	37 ± 1	$\frac{I_{308}}{I_{339}} = \frac{74}{26}$	Not graphed
	339 ± 1	13 ± 1		
	384 ± 1	28 ± 1		
	417 ± 1	26 ± 2		
	437 ± 3	12 ± 2		
	301 ± 3	11 ± 5		
	313 ± 2	24 ± 4		

	339 ± 1	13 ± 1		
	366 ± 3	9 ± 1		
	387 ± 1	23 ± 1		
	411 ± 3	15 ± 3		
	427 ± 2	19 ± 3		
	447 ± 4	7 ± 2		

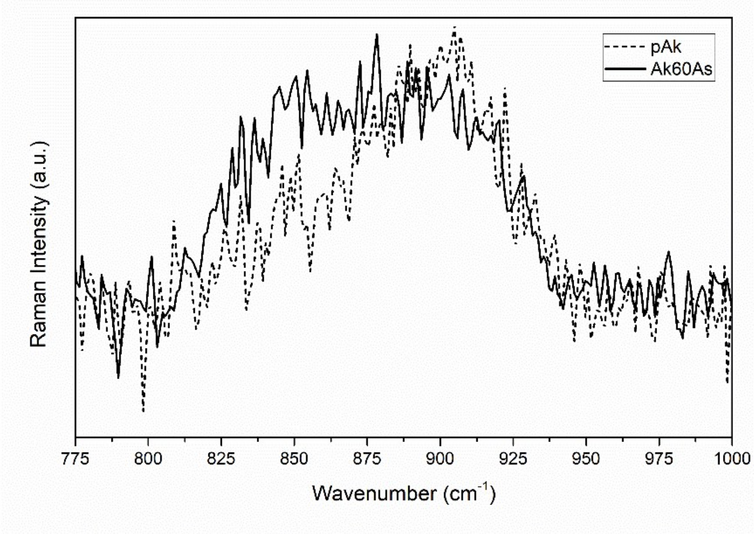

Figure SI_12. Raman spectra in the range from 775 and 1000 cm^{-1} for pure and co-precipitated with 60 ppm As^{5+} akaganeites.

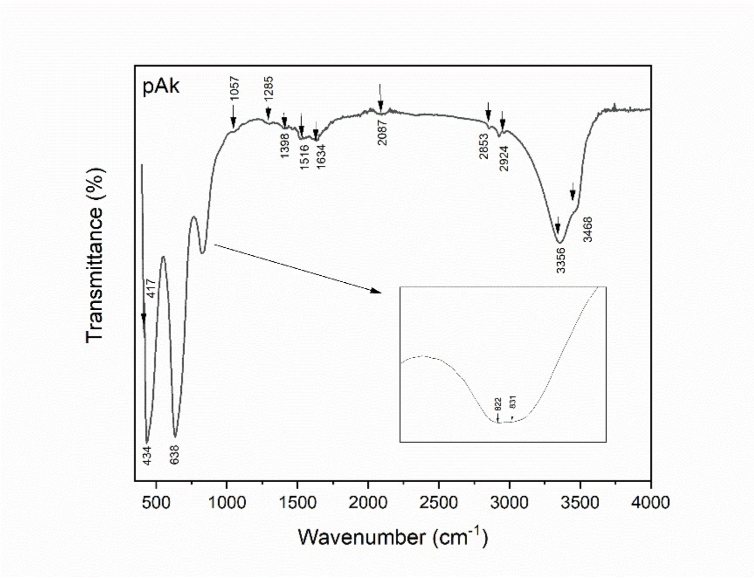

Figure SI_13. IR spectrum of pAk. The inset shows the region between 750 to 900 cm^{-1}.

Table SI_6. Wavenumbers of prominent bands observed in the infrared spectrum of pure akaganeite and compared with other studies. The table also includes the band assignments given by different authors.

Wavenumbers [cm^{-1}] of this study	**Wavenumbers [cm^{-1}] published in other studies**	**Band assignments given by different authors**
434 and 475	420 and 490 [54]	Symmetrical stretching vibrations of Fe-O in the octahedral site.[55] Translational modes of the FeO_6 octahedral unit.[56]
	Band from 439 to 491 [55]	
	420 and 481 (doublet) [56]	
638+670 (doublet)	650 [54]	Asymmetrical stretching vibrations of Fe-O-Fe [55]
	700 [55]	
	644+697 (doublet) [56]	
822+831 (doublet)	820+850 (doublet) [54]	Librations of linear and bifurcated O-H…Cl at the tunnels.[56]
	820+847 (doublet) [56]	
1516 and 1634	1630 [54]	OH and H_2O bending.[54]
	Band from 1630 to 1648 [55]	
3356+3468 (doublet)	3390+3480 (doublet) [54]	OH structural and molecular H_2O.[54] Vibration of linear and bifurcated O-H…Cl bonds.[56]
	3392-3458 (doublet) [56]	
	Broad band from 3430 to 3458 [55]	

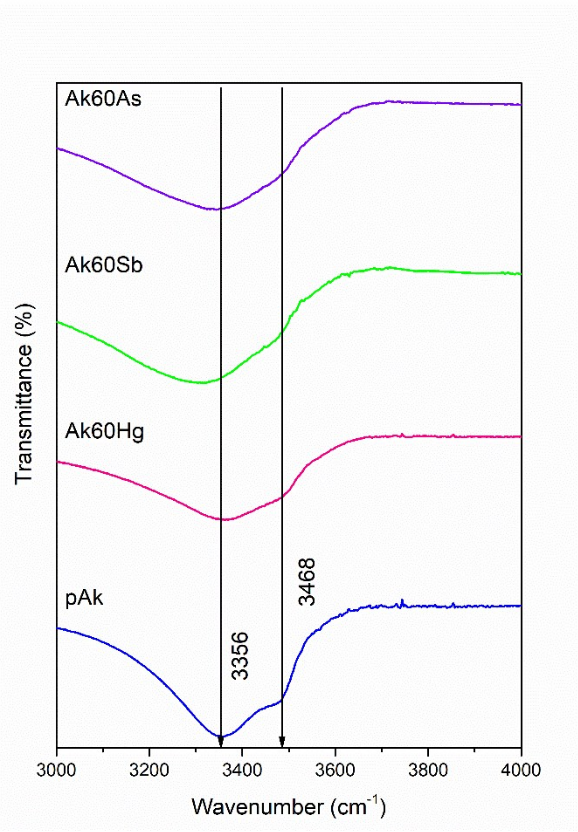

Figure SI_14. IR spectra of pAk, Ak60Hg, Ak60Sb and Ak60As in the wavenumber region from 3000 to 4000 cm^{-1}.

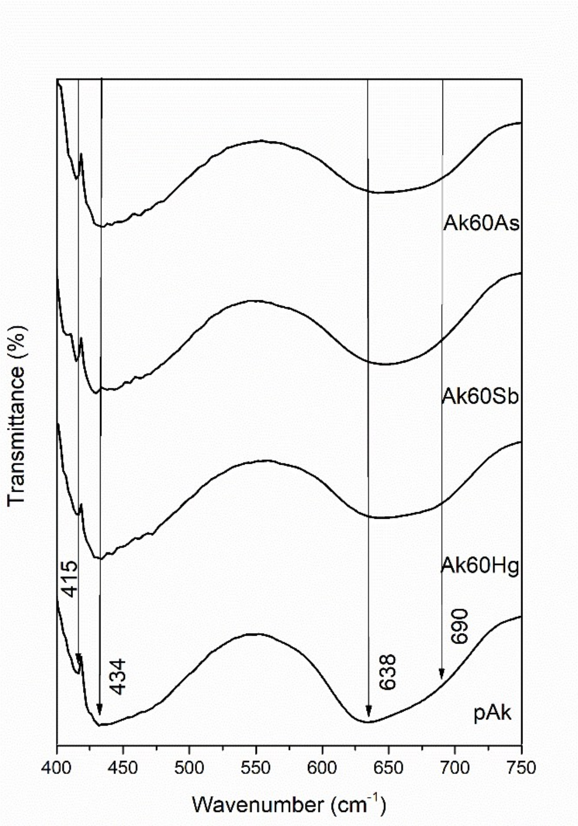

Figure SI_15. IR spectra of pAk, Ak60Hg, Ak60Sb and Ak60As in the wavenumber region from 400 to 750 cm^{-1}.

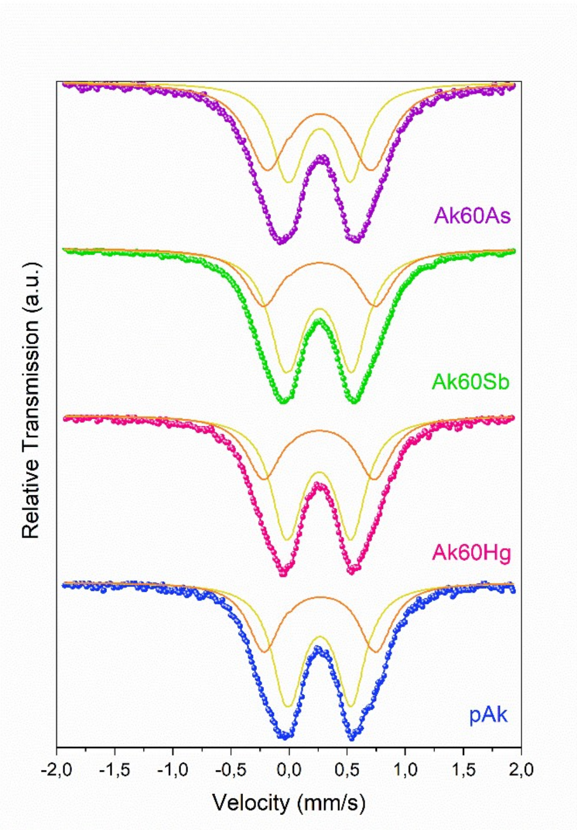

Figure SI_16. 300 K Mössbauer spectra of pAk, Ak60Hg, Ak60Sb and Ak60As.

Table SI_7. Refined values of hyperfine parameters resulting from the 300K and the 77K Mössbauer spectra of pure akaganeite: Isomer shift (δ), quadrupolar shift (2ε), quadrupolar splitting (Δ), linewidth (Γ/2), magnetic hyperfine field (B_{hf}) and relative absorption area (A).

T [K]	Components	δ [mm/s]	2ε or Δ [mm/s]	Γ/2 [mm/s]	B_{hf}[T]	Area [%]
300	D1	0.38±0.003	0.54±0.01	0.15±0.003	0	60
	D2	0.39±0.003	0.94±0.01	0.17±0.01	0	40
77	S1	0.50±0.01	-0.09±0.01	0.18±0.01	48.0±0.5	28
	S2	0.50±0.01	-0.09±0.01	0.18±0.01	46.5±0.6	28
	S3	0.47±0.01	-0.39±0.02	0.24±0.02	46.3±2.0	22
	S4	0.47±0.01	-0.39±0.02	0.24±0.02	44.0±1.2	22

Table SI_8. Refined values of hyperfine parameters resulting from the 300K Mössbauer spectra of akaganeites co-precipitated with Hg^{2+}, Sb^{3+} and As^{5+}. Isomer shift (δ), quadrupolar shift (2ε), quadrupolar splitting (Δ), linewidth (Γ/2), magnetic hyperfine field (B_{hf}) and relative absorption area (A).

Hg(II)					
Sample	**Components**	**δ [mm/s]**	**2ε [mm/s]**	**Γ/2 [mm/s]**	**Area [%]**
Ak20Hg	D1	0.38±0.002	0.54±0.01	0.17±0.004	60
	D2	0.38±0.003	0.93±0.02	0.19±0.01	40
Ak60Hg	D1	0.38±0.002	0.55±0.01	0.16±0.002	62
	D2	0.38±0.002	0.94±0.01	0.18±0.01	38
Sb(III)					
Ak10Sb	D1	0.38±0.003	0.55±0.01	0.16±0.003	63
	D2	0.38±0.003	0.97±0.01	0.16±0.01	37
Ak20Sb	D1	0.38±0.003	0.56±0.01	0.16±0.002	67
	D2	0.38±0.003	0.98±0.01	0.18±0.01	33
Ak60Sb	D1	0.38±0.002	0.54±0.00	0.17±0.002	65
	D2	0.38±0.003	0.95±0.01	0.18±0.003	35
As(V)					
Ak60As	D1	0.38±0.003	0.56±0.004	0.17±0.002	59
	D2	0.38±0.003	0.94±0.00	0.2±0.004	41

Table SI_9. Refined values of hyperfine parameters of the 77K Mössbauer spectra for akaganeites co-precipitated with Hg^{2+}. Isomer shift (δ), quadrupolar shift (2ε), hyperfine field (B_{hf}) and relative absorption area (A).

	S1				**S2**				**S3**				**S4**			
Sample	δ [mm/s]	2ε [mm/s]	B_{hf} [T]	Area [%] ±2	δ [mm/s]	2ε [mm/s]	B_{hf} (T)	Area [%] ±2	δ [mm/s]	2ε [mm/s]	B_{hf} [T]	Area [%] ±2	δ [mm/s]	2ε [mm/s]	B_{hf} [T]	Area [%] ±2
pAk	0.50 ±0.01	-0.09 ±0.01	48 ±0.5	28	0.50 ±0.01	-0.09 ±0.01	46.5 ±0.6	28	0.47 ±0.01	-0.39 ±0.02	46.3 ±2.0	22	0.47 ±0.01	-0.39 ±0.02	44.0 ±1.2	22
Ak5Hg	0.49 ±0.01	-0.09 ±0.01	47.9 ±0.5	27	0.49 ±0.01	-0.09 ±0.01	46.5 ±0.6	27	0.47 ±0.01	-0.38 ±0.02	46.2 ±2.1	23	0.47 ±0.01	-0.38 ±0.02	44.0 ±1.0	23
Ak20Hg	0.49 ±0.01	-0.10 ±0.01	47.9 ±0.5	28	0.49 ±0.01	-0.10 ±0.01	46.3 ±0.6	28	0.46 ±0.01	-0.39 ±0.02	45.9 ±1.9	22	0.46 ±0.01	-0.39 ±0.02	43.5 ±1.1	22
Ak60Hg	0.48 ±0.01	-0.13 ±0.01	47.2 ±0.5	30	0.48 ±0.01	-0.13 ±0.01	45.6 ±0.6	30	0.46 ±0.01	-0.40 ±0.02	45.1 ±1.7	20	0.46 ±0.01	-0.40 ±0.02	42.3 ±1.04	20

Table SI_10. Refined values of hyperfine parameters of the 77K Mössbauer spectra for akaganeites co-precipitated with Sb^{3+}. Isomer shift (δ), quadrupolar shift (2ε), hyperfine field (B_{hf}) and relative absorption area (A).

	S1				S2				S3				S4			
Sample	δ [mm/s]	2ε [mm/s]	B_{hf} [T]	Area [%] ±2	δ [mm/s]	2ε [mm/s]	B_{hf} (T)	Area [%] ±2	δ [mm/s]	2ε [mm/s]	B_{hf} [T]	Area [%] ±2	δ [mm/s]	2ε [mm/s]	B_{hf} [T]	Area [%] ±2
pAk	0.50 ±0.01	-0.09 ±0.01	48 ±0.5	28	0.50 ±0.01	-0.09 ±0.01	46.5 ±0.6	28	0.47 ±0.01	-0.39 ±0.02	46.3 ±2.0	22	0.47 ±0.01	-0.39 ±0.02	44.0 ±1.2	22
Ak20Sb	0.50 ±0.004	-0.13 ±0.01	47.8 ±0.4	35	0.50 ±0.004	-0.13 ±0.01	46.1 ±0.5	35	0.46 ±0.01	-0.33 ±0.03	45.6 ±1.4	15	0.46 ±0.01	-0.33 ±0.03	42.9 ±1.0	15
Ak60Sb	0.50 ±0.004	-0.14 ±0.01	47.2 ±0.5	30	0.50 ±0.004	-0.14 ±0.01	47.2 ±0.5	30	0.47 ±0.01	-0.34 ±0.04	45.1 ±1.6	20	0.47 ±0.01	-0.34 ±0.04	42.3 ±1.0	20

Table SI_11. Refined values of hyperfine parameters of the 77K Mössbauer spectra for akaganeites co-precipitated with As^{5+}. Isomer shift (δ), quadrupolar shift (2ε), hyperfine field (B_{hf}) and relative absorption area (A).

	S1				S2				S3				S4			
Sample	δ [mm/s]	2ε [mm/s]	B_{hf} [T]	Area [%] ±2	δ [mm/s]	2ε [mm/s]	B_{hf} (T)	Area [%] ±2	δ [mm/s]	2ε [mm/s]	B_{hf} [T]	Area [%] ±2	δ [mm/s]	2ε [mm/s]	B_{hf} [T]	Area [%] ±2
pAk	0.50 ±0.01	-0.09 ±0.01	48 ±0.5	28	0.50 ±0.01	-0.09 ±0.01	46.5 ±0.6	28	0.47 ±0.01	-0.39 ±0.02	46.3 ±2.0	22	0.47 ±0.01	-0.39 ±0.02	44.0 ±1.2	22
Ak5As	0.49 ±0.01	-0,09 ±0,01	48.0 ±0.5	27	0.49 ±0.01	-0,09 ±0,01	46.7 ±0.6	27	0.46 ±0.01	-0.39 ±0.02	46.3 ±1.9	23	0.46 ±0.01	-0.39 ±0.02	44.1 ±1.0	23
Ak20As	0.49 ±0.01	-0.11 ±0.01	47.9 ±0.5	30	0.49 ±0.01	-0.11 ±0.01	46.4 ±0.5	30	0.46 ±0.01	-0.41 ±0.02	46.0 ±1.6	20	0.46 ±0.01	-0.41 ±0.02	43.6 ±0.9	20
Ak60As	0.48 ±0.01	-0.14 ±0.01	46.7 ±0.7	27	0.48 ±0.01	-0.14 ±0.01	44.9 ±0.8	27	0.45 ±0.01	-0.28 ±0.02	44.2 ±2.5	23	0.45 ±0.01	-0.28 ±0.02	41.1 ±1.5	23

Table SI_12. Linewidths of the four sextet components of the 77 K Mössbauer spectra for the coprecipitated samples with Hg^{2+}, Sb^{3+} and As^{5+}.

	S1	**S2**	**S3**	**S4**
Sample	**Γ/2 [mm/s]**	**Γ/2 [mm/s]**	**Γ/2 [mm/s]**	**Γ/2 [mm/s]**
pAk	0.18±0.01	0.18±0.01	0.24±0.02	0.24±0.02
Ak5Hg	0.20±0.01	0.20±0.01	0.25±0.01	0.25±0.01
Ak20Hg	0.21±0.01	0.21±0.01	0.27±0.01	0.27±0.01
Ak60Hg	0.22±0.01	0.22±0.01	0.26±0.01	0.26±0.01
Ak20Sb	0.22±0.01	0.22±0.01	0.22±0.01	0.22±0.01
Ak60Sb	0.21±0.01	0.21±0.01	0.25±0.02	0.25±0.02
Ak5As	0.18±0.01	0.18±0.01	0.24±0.01	0.24±0.01
Ak20As	0.19±0.01	0.19±0.01	0.23±0.01	0.23±0.01
Ak60As	0.21±0.01	0.21±0.01	0.30±0.02	0.30±0.02